



Supporting Online Material for

**Multistep Synthesis of a Radiolabeled Imaging Probe Using Integrated
Microfluidics**

Chung-Cheng Lee, Guodong Sui, Arkadij Elizarov, Chengyi Jenny Shu, Young-Shik Shin, Alek N. Dooley, Jiang Huang, David Stout, Hartmuth C. Kolb, Owen N. Witte, Nagichettiar Satyamurthy, James R. Heath, Michael E. Phelps, Stephen R. Quake,*
Hsian-Rong Tseng*

*To whom correspondence should be addressed. E-mail: quake@stanford.edu;
hrtseng@mednet.ucla.edu

Published 16 December 2005, *Science* **310**, 1793 (2005)
DOI: 10.1126/science.1118919

This PDF file includes:

Materials and Methods

Figs. S1 to S7

Movie S1

References

Materials and Methods.

Fabrication of the first generation chemical reaction circuits. The chip was fabricated using multi-layer soft lithography. (1, 2) Two different molds were first fabricated by photolithographic processes to create the fluidic channels and the control channels for actuating the valves located in the respective layers of the PDMS-based chemical reaction circuits. The mold used to create the fluidic channels was made by a two-step photolithographic process. In the first step, a 45- μm thick negative photoresist (SU8-2025) was spin coated on to a silicon wafer (Silicon Quest, San Jose, USA). After UV exposure and development, a square-profiled pattern for the miniaturized anion exchange column was obtained. In the next step, a second layer of 45- μm thick positive photoresist (AZ 100XT PLP) was spin coated on the same wafer. Prior to the UV exposure the mask was aligned (Karl Suss America Inc., Waterbury, VT) to ensure a good match between the control and fluid channel patterns. Once the positive photoresist was developed, the wafer was heated above the glass transition temperature of the positive photoresist. As a result, the surface profile of the patterned positive photoresist was transformed into a round profile while the profile of the negative photoresist remained unchanged (square profile). This device has a channel height of 45 μm and width of 200 μm . The control channels mold was made by fabricating a 25 μm -thin negative photoresist (SU8-2025) pattern on a silicon wafer. In order to achieve reliable performance of each valve, the width of the control channel was set at 250 μm in sections where the valve modules are located.

Before fabricating the device, both the fluidic and control molds were exposed to trimethylchlorosilane (TMSCl) vapor for 2-3 minutes. Well-mixed PDMS (GE, RTV 615 A and B in 5:1 ratio) was poured onto the fluidic mold located in a Petri dish to give a 5 mm-thick

fluidic layer. Another portion of PDMS (GE, RTV 615 A and B in 20:1 ratio) was spin-coated onto the control mold (1600 rpm, 60 s, ramp 15 s) to obtain the control layer. The thick fluidic layer and thin control layer were cured in an 80 °C oven for 50 minutes. After incubation, the thick fluidic layer was peeled off the mold, and holes were punched onto the fluidic layer for access of reaction solutions. The fluidic layer was then trimmed, cleaned and aligned onto the thin control layer. After baking at 80°C for 60 minutes, the assembled layer was peeled off the control mold, and another set of holes were punched for access to control channels. These assembled layers were then placed on top of a glass slide that was coated (1600 rpm, 60 s, ramp 15 s) with PDMS (GE RTV 615 A and B in 20:1 ratio) that had been cured for 45 minutes in the oven. The device was complete after overnight incubation.

Control interface. The pneumatic control setup consists of 4 sets of eight-channel manifolds controlled through BOB3 breakout controller board (Fluidigm, San Francisco, USA). Argon gas that was pre-dried through a gas purifier (Hammond Drierit, Xenia, USA) provides pressure (30 psi) to the manifolds. 32 Control lines from the device are individually connected to the corresponding channels on the manifolds with metal pins (23 Gauge, New England Small Pin Corp, USA) using Tygon microbore tubing (Cole-Parmer East, Bunker Court, USA). When a channel on the manifold is activated, argon gas enters the control line connected to the specific channel, providing pressure to close valves in the microfluidic device. The control interface was created using Labview program on a PC. A digital I/O card (AT-DIO-32HS National Instruments) digitally controls the switching of manifolds through the BOB3 breakout controller board. The Labview program allows for manual control of individual valves and for automation of the synthesis processes.

Materials. All reagents were purchased from Sigma-Aldrich. Solvents purchased from VWR/EMD were purified according to literature procedure. (3) GC-MS was performed with GC/EI Time-of-Flight mass spectrometer (Micromass GCT). DBS-MS capillary column (40 m long, 320 μ m of OD) was employed for GC analyses of [19]FDG intermediate (**2b**) and product (**3b**) using Helium as carrier gas at flow rate of 1.2 mL/min. No-carrier-added [18 F]fluoride (specific activity: > 10,000 Ci/mmol) was produced by 11 MeV proton bombardment of 95% 18 O-enriched H₂O via $^{18}\text{O}(\text{p},\text{n})^{18}\text{F}$ nuclear reaction using a RDS-112 cyclotron. HPLC analysis was performed using a Rainin-HP system equipped with a γ -detector. A Phenomenex column (Econosphere-NH₂, 5 μ m, 250 \times 4.6 mm) was used with a solvent system of 85% MeCN and 15% H₂O. Radio-TLC analysis was performed on silica plate (EM Separation Technology, Silica gel 60) with eluent system of 85% MeCN and 15% H₂O.

Preparation and evaluation of anion exchange column. Anion exchange beads (Source 15Q, Amersham Biosciences) were packed into the column module by introducing an aqueous solution containing suspended beads into the microfluidic chamber. The beads were activated by passing 1.0 M of KHCO₃ through the column followed by sequential introduction of DI water (18 M Ω).

Snapshots of FDG synthesis in the chemical reaction circuits. The FDG (**3a,b**) synthesis in the circuit is based on three sequential synthetic processes starting from (i) concentration of dilute fluoride, followed by (ii) fluorine substitution reaction of the D-mannose triflate precursor **1** and (iii) acidic hydrolysis of the fluorinated intermediate **2a** (or **2b**). There were 15 steps to

complete the FDG (**3a,b**) synthesis in a circuit. We summarize the details of these sequential operations using schematic diagrams shown in Figures S1-S3.

GC-MS analysis of the fluorinated intermediate 2b and [¹⁹F]FDG (3b). The fluorinated intermediate **2b** produced in the circuit was analyzed by GC-MS, which indicated that the conversion yield for the fluorination reaction was about 95%. (Fig S4b) Due to the low volatility of [¹⁹F]FDG (**3b**), the [¹⁹F]FDG (**3b**) obtained in the circuit had to be first treated by TMSCl prior to the GC-MS analysis. The GC-MS result indicated that the hydrolytic reaction of intermediate **2b** results [¹⁹F]FDG (**3b**) with > 90% purity. (Fig. S4C)

1,3,4,6-Tetra-*O*-acetyl-2-[¹⁹F]fluoro-2-deoxy-D-glucose (2b). A 40 nL anhydrous MeCN solution containing 1,3,4,6-tetra-*O*-acetyl-2-*O*-trifluoromethanesulfonyl-D-manno-pyranose (mannose triflate) (**1**) (92 ng, 1.9×10^{-10} mol) and 4,7,13,16,21,24-hexaoxa-1,10-diazabicyclo [8,8,8]hexacosane (Kryptofix 222) (364 ng, 9.6×10^{-10} mol) was introduced into the reaction loop containing the dried KF (which was concentrated by the earlier fluoride concentration process). After all the valves around the reaction loop were closed, the circuit was heated at 100 °C for 30 seconds and maintained at 120 °C for 50 seconds. Meanwhile, the circulating pump was turned on to provide efficient mixing. After the chip was cooled down to 35 °C, the reaction residue inside the loop was flushed out with MeCN for GC-MS analysis. Although we can not obtain an accurate reaction yield from GC-MS analysis it is obvious that the entire D-mannose triflate precursor **1** disappeared after the reaction and the fluorinated intermediate **2b** was the only reaction product. (Fig. S4B)

2-Deoxy-2-[¹⁹F]fluoro-D-glucose ([¹⁹F]FDG) (3b). After the fluorination step, 40 nL of HCl solution (3.0 N) was loaded into reaction loop. With all the valves closed and circulating pump running, the hydrolysis of the fluorinated intermediate **2** was finished in 1 minute at a temperature of 60 °C. After cooling down to 35 °C, the final product, [¹⁹F]FDG (**3b**) was flushed out from the circuit by water. Final aqueous solution was removed *in vacuo*. Due to the low volatility, [¹⁹F]FDG (**3b**) was derivatized with TMSCl prior to GC-MS analysis. The GC-MS result indicated that the hydrolytic reaction of intermediate **2b** results [¹⁹F]FDG (**3b**) with > 90% purity. (Fig. S4C)

2-Deoxy-2-[¹⁸F]fluoro-D-glucose ([¹⁸F]FDG) (3a). 720 μCi of [¹⁸F]fluoride in ca. 1 μL of [¹⁸O]water was introduced into the fluoride concentration loop of the circuit. Because a relatively high loading rate (65 nL/sec) was applied, only 500 μCi of [¹⁸F]fluoride (limiting reagent) was trapped in the column. An 18 nL of K₂CO₃ solution (0.25 M, 4.5x10⁻⁹ mole) was introduced to fill the rectangular loop, and the circulating pump module was then turned on so that the K₂CO₃ solution could loop through the column continuously to elute a concentrated [¹⁸F]KF solution. After circulation, 20 nL of K₂CO₃ solution was introduced into fluoride concentration loop to displace the concentrated [¹⁸F]fluoride solution into the ring-shaped reaction loop. With all the valves around reaction loop closed, the circuit was heated on a digitally controlled hotplate. The circuit was cooled down to 35 °C within 1 minute, and anhydrous MeCN (40 nL) was introduced into the reaction loop. The circuit was heated again to remove the water residue inside the loop. Kryptofix 222 (1.4 μg, 3.7 x 10⁻⁷ mol) and the mannose triflate **1** (324 ng, 6.7 x 10⁻¹⁰ mol) in anhydrous MeCN were introduced into the reaction loop. The circuit was heated with a gradient (100 °C/30 seconds, 120 °C/50 seconds). At

the same time, the solution was actively mixed by the circulating pump to give [^{18}F]fluorinated intermediate **2a** in the circuit. After cooling the circuit down to 35 °C within 1 minute, HCl aqueous solution (3.0 N) was introduced into the reaction loop. The mixture was mixed by the circulating pump for 1 min at 60 °C. In this step, the intermediate **2a** was hydrolyzed to yield the final product [^{18}F]FDG (**3a**). After cooling down to room temperature, the final product, 190 μCi of [^{18}F]FDG (**3a**) (38% yield) was flushed out from the chip by water for the analyses of radio-TLC and radio-HPLC. The analyses of radio-TLC (Fig. S5) and radio-HPLC suggested that the unpurified mixture obtained upon the sequential production of [^{18}F]FDG (**3a**) has a radiochemical purity of 97.6 %.

Fabrication of the second generation chemical reaction circuits. The second generation chemical reaction circuits (Fig. S6) were manufactured by a soft lithography method similar to the one described above. (Fabricated at Fluidigm Corp.) The main differences are (i) a third vent layer is located above the fluidic and control layers, (ii) all three layers of the circuit were made from 10:1 A/B PDMS and are held together by placing a 1- μm thick layer of PDMS B component between every two layers and (iii) the assembled device was mounted on a 2-inch silicon wafer. The dimensions of the arched flow channels are 250- μm wide and 45- μm tall. Only the water inlet channel is 300 μm wide. The reaction chamber is 5 mm in diameter and 250 μm in height (with a total volume of 5 μL). The control channels form 250 x 250 μm intersections with flow channels. The vent is in the third layer with channels located 50 μm above the reaction chamber 250 μm apart from each other and measuring 250 x 250 μm in cross-section.

Chip II description and Logic: In order to increase the amount of [^{18}F]FDG (**3a**) produced by a circuit to human dosage levels, the second generation circuits were developed. Key features include (i) a 5- μL coin-shaped reactor, (ii) an overlaying vent channel connected to an external vacuum line, (iii) an external ion exchange column controlled by valves on the circuit, and (iv) a manifold for introducing the mannose triflate. The geometry of reactor inlets/outlets determines the fluid dynamics inside the circuit leading to better mixing during the reaction. The architecture of the new circuit also minimizes the number of valves. Currently the largest [^{18}F]FDG (**3a**) dose produced by this chip in a single run equals 1.74 mCi. This chip was used to generate [^{18}F]FDG (**3a**) for the mouse image presented in Figure 4B. The vacuum vent is advantageous during the solvent exchange steps. Full operation of the chip during [^{18}F]FDG (**3a**) synthesis is described in Figure S7. [^{18}F]FDG (**3a**) is eluted as an acidic solution with 96 % purity, which is first neutralized by 1.0 M NaHCO_3 and then passed through an alumina column (190 mg) to remove residual fluoride. The resulting solution exhibits 99 % [^{18}F]FDG (**3a**) purity according to radio-TLC (Fig. 4A).

Chemical reaction circuits II: Off-chip fluoride concentration. For the operation of the new generation circuit, the [^{18}F]fluoride concentration was carried using the automatic Explora RN Nucleophilic [^{18}F]Fluorination System (Siemens Biomarker Solutions, Culver City, CA). An MP-1 resin cartridge was used to trap the dilute fluoride obtained from cyclotron. The activity was eluted with a solution of K_2CO_3 (3 mg) in water (400 μL). Upon water evaporation, the solution of Kryptofix 222 (20 mg) in MeCN (400 μL) was added followed by solvent evaporation. The residue was dissolved in anhydrous MeCN (200 μL) and the resulting solution

of [^{18}F]Fluoride / K_2CO_3 / K222 in MeCN containing 700 mCi of [^{18}F]fluoride was transferred from the Explora system via approximately 2 m of tubing to a conical vial (source vial) located near the CRi. Application of 10 psi of pressure to the source vial introduced concentrated [^{18}F]Fluoride / K_2CO_3 / K222 / MeCN solution into the circuit.

Compatibility of Elastomers: CRC II has been designed to produce up to 100 mCi of FDG. The low yield reported here is explained by the reaction of the major part of [^{18}F]fluoride with PDMS, quantified by placing a charcoal trap in the vacuum line. The work is in progress to alternative elastomers for the chip fabrication. One of them is based on perfluoropolyether (PFPE). It has been validated with bulk experiments, where flakes of elastomer (200 mg) in a vial are exposed to the fluorination conditions similar to those used on the chip, i.e. solvent evaporation (under vacuum) from concentrated [^{18}F]fluoride / K_2CO_3 / K222 / MeCN solution (300 μL). In case of PDMS 21 % of fluoride was incorporated into volatile products, whereas in case of PFPE that number was 0.04%. This result suggests that once the fabrication of PFPE chips is optimized, the loss of fluoride during FDG synthesis will be minimized and the yield should improve dramatically.

Mouse model. The tumor model used was a strongly immunogenic, non-metastasizing retrovirally-induced rhabdomyosarcoma (M-MSV/M-MuLV). (4) MSV is a replication-defective, acutely transforming retrovirus carried with helper activity provided by M-MuLV, which encodes the gag, pol, and env components that are necessary for cell infection and replication. (5) Rhabdomyosarcomas develop at the intramuscular inoculation site after a short latency period (7-10 days) and regress over a period of 4-5 wk following the induction of a strong immune

reaction in immunocompetent adult mice. These lesions were characterized by a mixture of virus-infected myocytes and a large infiltrate of lymphocytes, granulocytes, and macrophages. Both cellular and humoral immune responses induced are dependent on presentation by *H-2 D^b* alleles. (6) Rejection was mediated by CD8⁺ cytolytic T cells, which recognize peptides from the gag and env proteins of M-MuLV, and requires help from CD4⁺ T cells. (7-8)

Mouse imaging. The tumor bearing mouse was injected with 272 microCi of FDG via its tail vein. Following 1-h uptake and non-specific clearance, the mouse was imaged for 15 minutes in a Focus 220 microPET, followed by a microCT scan (Siemens, Knoxville, TN). MicroPET and microCT images were reconstructed using MAP and Fledkamp to resolutions of 1.2 mm and 0.4 mm respectively, and then fused using AMIDE image visualization software.

Figure Captions

Figure S1. Schematic diagrams summarize the fluoride concentration process which consisted of 9 steps in the circuit. (A) Diluted fluoride solution (indicated in blue) was introduced into the fluoride concentration loop from the top-left channel on the chip. The fluoride ions were trapped by anion exchange beads in the column. The filtrate solution was exported out of the device through the waste channel. The loading speed of fluoride solution was controlled by the metering pump (labeled in yellow). The loading process took around 2 min. (B) Following fluoride loading, 18 nL of K_2CO_3 solution (0.25 M) was pumped into fluoride concentration loop from the left-middle channel. This step takes 6 seconds at 25 °C. (C) The K_2CO_3 solution was circulated in the fluoride concentration loop for 2 minutes to assure all the fluoride trapped on beads was released into the solution. By the end of this step, the fluoride concentration within the loop can increase by two orders of magnitude compared to the concentration of loaded fluoride solution. (D) After circulation, 20 nL of K_2CO_3 solution was introduced into the fluoride concentration loop to displace the concentrated fluoride solution into the reaction loop. This dead-end filling process (all the valves are closed except the valve controlling the loading channel, the air inside the loop is pushed out through the porous PDMS matrix) took 20 seconds. (E) With all the valves around reaction loop closed, the circuit was heated on a digitally controlled hotplate with a gradient (100 °C for 30 seconds, 120 °C for 30 seconds, 135 °C for 3 minutes). Most of the water from the concentrated fluoride solution was removed through direct evaporation. (F) The circuit was cooled down to 35 °C within 1 minute. (G) Anhydrous MeCN (in green) was

introduced into the reaction loop through the bottom middle channel by dead-end filling. This step took less than 20 seconds at 25 °C. (H) The circuit was heated again with a gradient (80 °C/30 seconds, 100 °C/1 minutes) to remove the remaining water inside the loop. With all valves around the loop closed, MeCN and water vapors were removed through direct evaporation. (I) The circuit was cooled down to 35 °C within 40 seconds.

Figure S2. Schematic diagrams summarize the fluorine substitution process which is composed of 3-step sequential operations in the circuit. (A) Kryptofix 222 / the mannose triflate **1** in anhydrous MeCN were introduced from the top middle channel to the reaction loop by dead-end filling. This step took 20 seconds at 25 °C. (B) The circuit was heated with a gradient (100 °C/30 seconds, 120 °C/50 seconds). At the same time, the solution was actively mixed by the circulating pump. The fluorinated intermediate **2a** (or **2b**) was obtained by the end of this step. (C) The circuit was cooled down to 35 °C within 40 seconds.

Figure S3. Schematic diagrams summarize the hydrolytic process which is composed of 3-steps sequential operations in the circuit. (A) HCl aqueous solution (3.0 N) was introduced from the top right channel (in light blue) to the reaction loop by dead-end filling. This step took 20 seconds at 25 °C. (B) The HCl and the fluorinated intermediate **2a** (or **2b**) were mixed by the circulating pump for 1 minute at 60 °C. In this step, the intermediate **2** (or **2b**) was hydrolyzed to yield the final product FDG (**3a,b**). (C) The solution containing FDG (**3a,b**) (in dark blue) was flushed out of the device through the product line located at the bottom of the circuit.

Figure S4. (A) GC-MS plot of a mixture containing MeCN, mannose triflate **1** and Kryptofix 222. The two peaks at retention times of 14.73 and 18.10 min correspond to mannose triflate **1** and Kryptofix, respectively. (B) GC-MS plot of the mixture in (A) after its reaction with concentrated fluoride in the circuit. The peak having a retention time of 14.16 min corresponds the formation of the fluorinated intermediate **2b**. A calibrated integration of the chromatogram suggests a conversion yield of 95%. (C) GC-MS plot of a TMS-functionalized [^{19}F]FDG (**3b**) which is obtained by treating crude [^{19}F]FDG (**3b**) with TMSCl. The calibrated integration indicates that the hydrolytic reaction of intermediate **2b** resulted [^{19}F]FDG (**3b**) in > 90% purity.

Figure S5. Analytical TLC profile of the unpurified mixture obtained upon the sequential production of [^{18}F]FDG (**3a**) in the first generation circuit indicating that the radiochemical purity of the FDG production is up to 97.3 %. The two peaks with values for R_f of 0.0 and 0.4 correspond to [^{18}F]fluoride and [^{18}F]FDG (**3a**), respectively.

Figure S6. (A) A second generation circuit is in action for the [^{18}F]FDG (**3a**) production. (B) Schematic representation of the second generation circuit composed of three major functional components, including (i) vent channel, (ii) coin-shaped reactor and (iii) manifold for introduction of the mannose triflate **2a** solution.

Figure S7. Schematic diagrams summarized the [^{18}F]FDG (**3a**) synthesis on the second generation circuit. (A) Concentrated mixture of $^{18}\text{F}^-$ /Kryptofix222/ K_2CO_3 in MeCN is

introduced into the reaction chamber until the reaction chamber is 2/3 full. This process is accelerated by applying vacuum to the vent above the reaction chamber to remove the gas being displaced by the fluoride solution. (B) The mannose triflate **2a** solution in MeCN (25 mg/mL) is loaded to fill the distribution manifold by dead-end filling. The manifold is designed to introduce mannose triflate **2a** solution into the reaction chamber equally and simultaneously through the six ports. (C) The mannose triflate **2a** solution is introduced into the reaction chamber by employing 10 psi of loading pressure. (D) The reaction mixture was kept at 25 °C for 5 min, and the fluorination reaction is carried out at 65 °C for 2 min. The vacuum in the vent is then turned on to evaporate ¼ of MeCN in the reaction chamber. (E) 3N HCl solution is loaded into the reaction chamber, and the acidic hydrolysis is performed at 60 °C. (F) The remaining MeCN is evaporated at 75 °C for 5 min. (G) The reaction chamber is cooled to 40 °C and vacuum in the vent is turned off prior to elution. (H) As the valves are opened on the water inlet and the product outlet, [¹⁸F]FDG (**3a**) is flushed out of the chamber. The tangential inlet and outlet allow the water trajectory to follow along the far wall of the reaction chamber ensuring complete product elution.

Movie S1. The complete 14-min synthesis of FDG inside the circuit (time compressed).

REFERENCES

1. J. C. McDonald *et al.*, *Electrophoresis* **21**, 27 (2000).
2. M. A. Unger, H. P. Chou, T. Thorsen, A. Scherer, S. R. Quake, *Science* **288**, 113 (2000).
3. W. L. F. Armarego, C. L. L. Chai, *Purification of Laboratory Chemicals* (Butterworth Heinemann, New York, ed. Fifth, 2003).
4. Fefer, A., J.L. McCoy, and J.P. Glynn, *Cancer Res.* **27** (9), 1626 (1967).
5. Gorczynski, R.M. and R.A. Knight, *Eur. J. Immunol.* **5** (2), 148 (1975).
6. Milan, G., et al., *J Virol.* **73** (3), 2280 (1999).
7. Flyer, D.C., S.J. Burakoff, and D.V. Faller, *J. Immunol.* **147** (7), 2284 (1991).
8. Schepers, K., et al., *J. Immunol.* **169** (6), 3191 (2002).

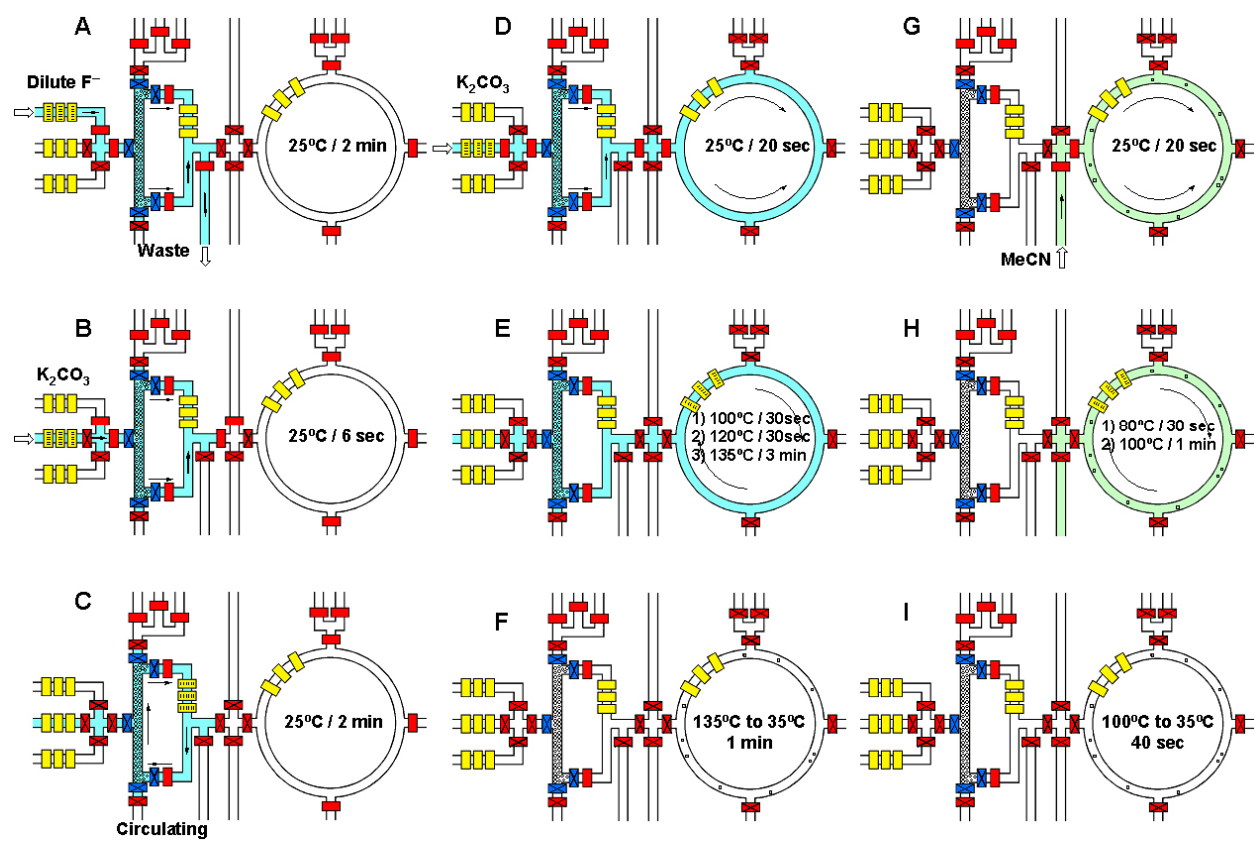


Figure S1

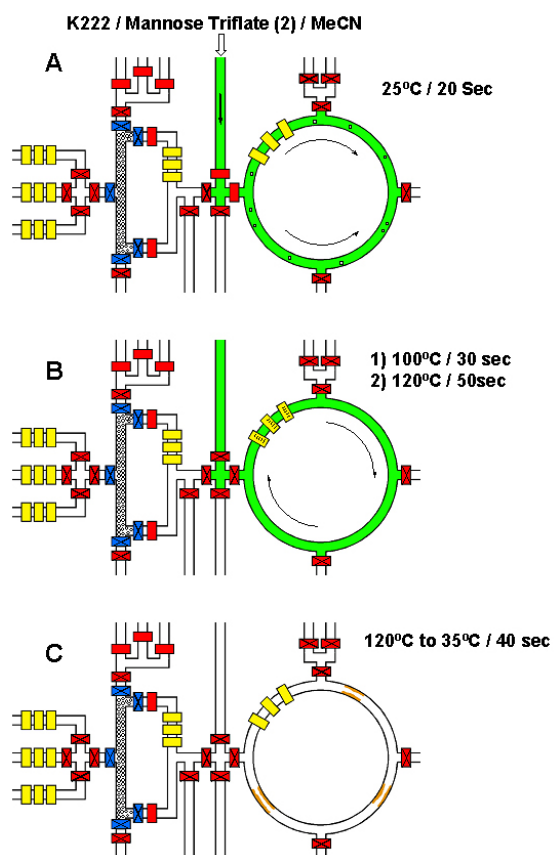


Figure S2

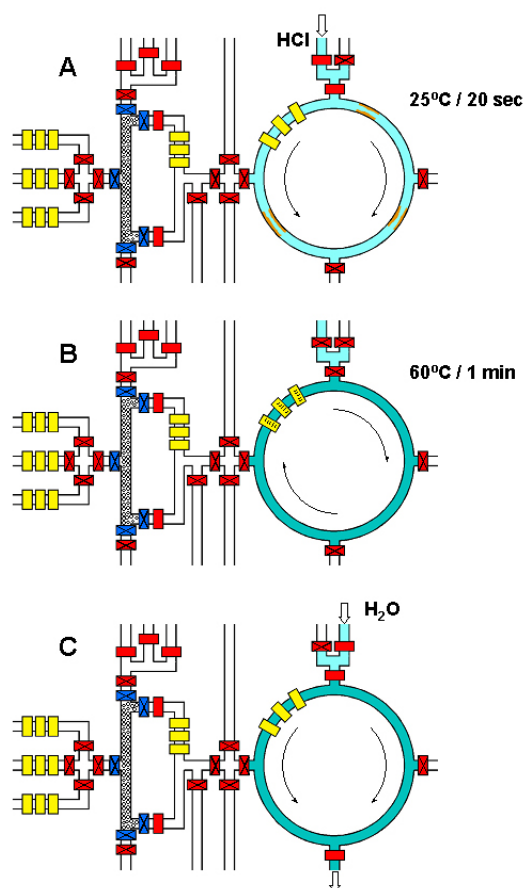


Figure S3

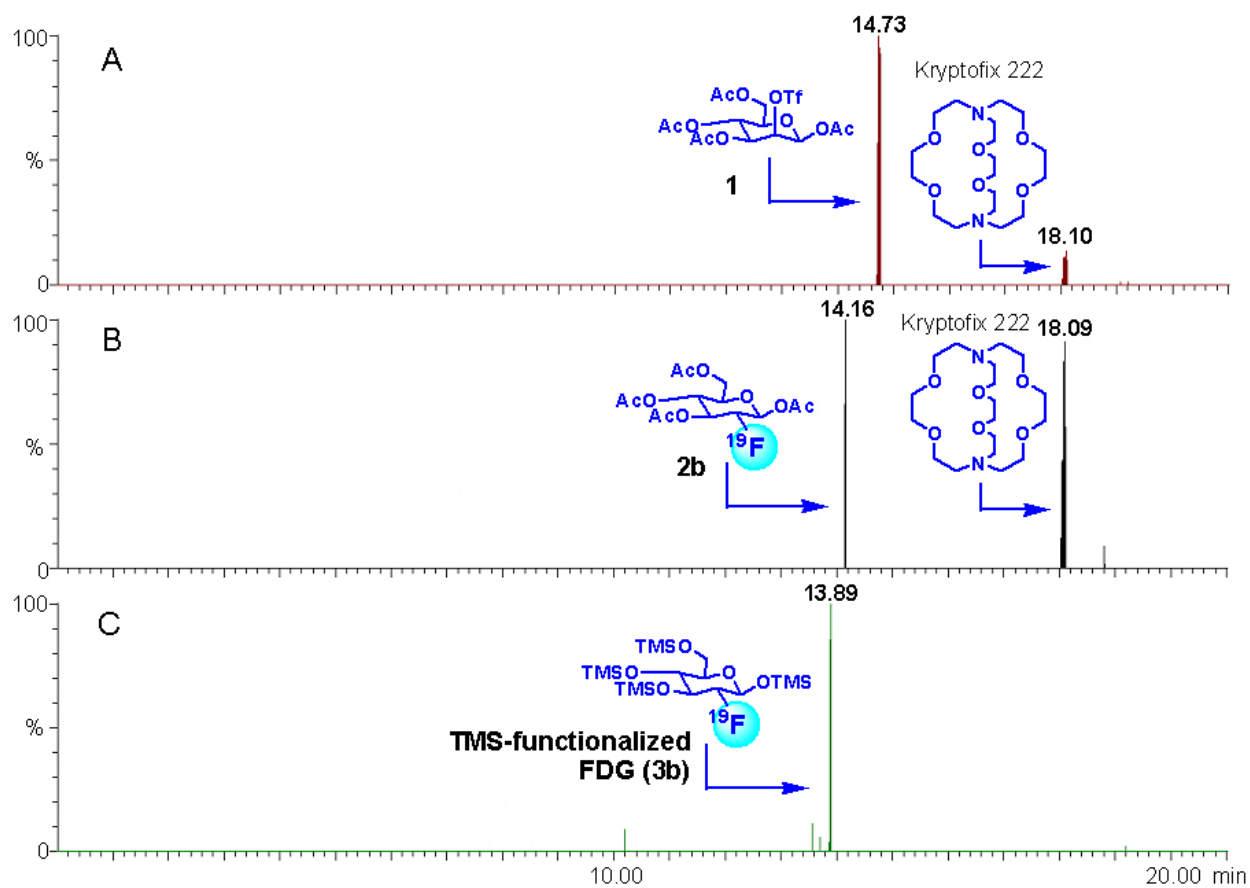


Figure S4

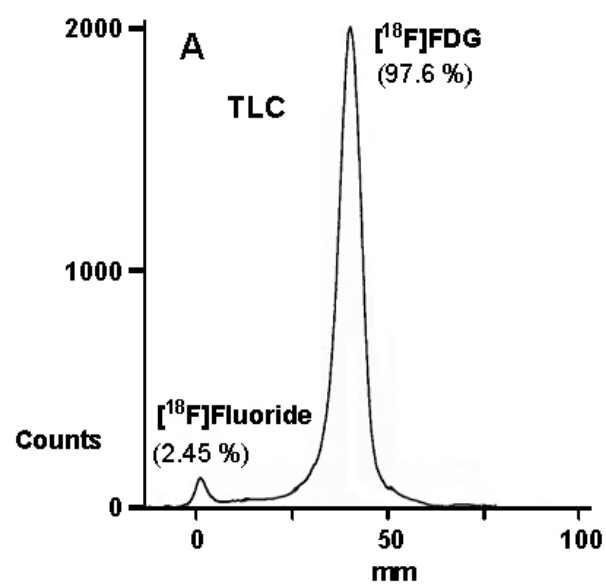


Figure S5

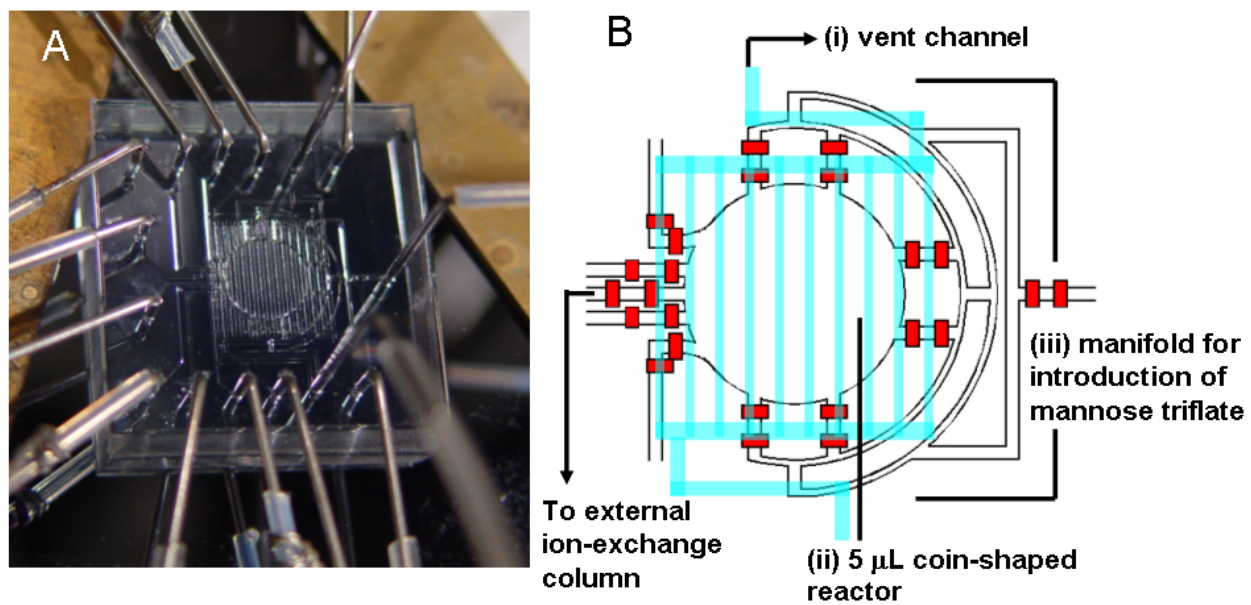


Figure S6

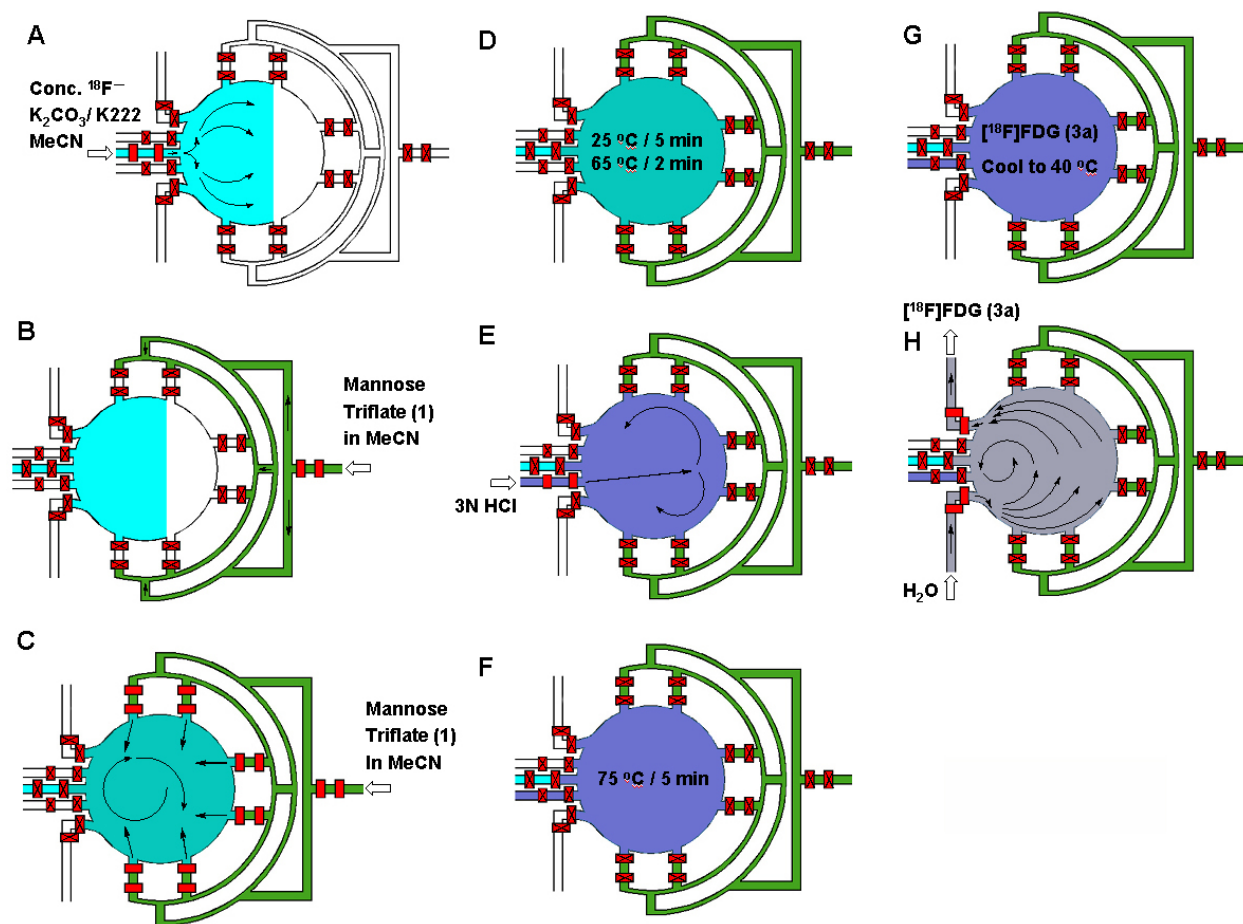


Figure S7